ELSEVIER

International Journal of Solids and Structures 41 (2004) 731–743

INTERNATIONAL JOURNAL OF SOLIDS and STRUCTURES

www.elsevier.com/locate/ijsolstr

Fracture analysis of a functionally graded interfacial zone under plane deformation

Gan-Yun Huang [a], Yue-Sheng Wang [a,*], Shou-Wen Yu [b]

[a] *Institute of Engineering Mechanics, Northern Jiaotong University, Beijing 100044, PR China*
[b] *Department of Engineering Mechanics, Tsinghua University, Beijing 100084, PR China*

Received 11 June 2003; received in revised form 6 August 2003

Abstract

A new multi-layered model for fracture analysis of functionally graded materials (FGMs) with the arbitrarily varying elastic modulus under plane deformation has been developed. The FGM is divided into several sub-layers and in each sub-layer the shear modulus is assumed to be a linear function while the Poisson's ratio is assumed to be a constant. With this new model, the problem of a crack in a functionally graded interfacial zone sandwiched between two homogeneous half-planes under normal and shear loading is investigated. Employment of the transfer matrix method and Fourier integral transform technique reduce the problem to a system of Cauchy singular integral equations. Stress intensity factors of the crack are calculated by solving the equations numerically. Comparison of the present new model with other existing models shows some of its advantages.

Keywords: Functionally graded materials; Interfacial zone; Fracture; Plane deformation; Stress intensity factors

1. Introduction

The conventional composites in general are of discrete, piecewise nature with sharp interfaces. The apparent mismatch in thermo-mechanical properties of the constituent materials may cause high residual and thermal stresses on the interface and thus make them one of the main failure sources. To improve the interfacial bonding strength and take the composite technology to full advantages, the newly developed functionally graded materials (FGMs) with continuously varying properties have been intentionally introduced as interfacial zones. Since Delale and Erdogan (1983), Eischen (1987) and Jin and Noda (1994) have proposed and verified the square root character of the crack tip singular field in non-homogeneous materials with continuously varying elastic modulus, many authors have been motivated to fracture analysis of FGMs by directly adopting the concepts developed for fracture analysis of homogeneous materials. Among them Erdogan and co-workers together with other authors used the model of the

* Corresponding author. Tel.: +86-10-51688417; fax: +86-10-51682094.
E-mail address: yswang@center.njtu.edu.cn (Y.-S. Wang).

0020-7683/$ - see front matter
doi:10.1016/j.ijsolstr.2003.08.007

exponential function to simulate the elastic modulus (it will be referred to as Erdogan's model in this paper) and have investigated a series of crack problems in functionally graded interfacial zones (e.g., Delale and Erdogan, 1988; Erdogan et al., 1991; Ozturk and Erdogan, 1993, 1995, 1996; Fildis and Yahsi, 1996, 1997; Choi et al., 1998; Shbeeb and Binienda, 1999). Wang et al. (1996) used the power-law function to describe the FGMs' properties, while Gao (1991) and Ergüven and Gross (1999) employed the perturbation approach to study the crack problem of non-homogeneous materials with properties of slight variation. However, one of the obvious shortcomings for all those methods is that they cannot be used for the FGMs with properties of arbitrary variation. Wang et al. (2000) and Itou (2001) used a piecewise multi-layered model (PWML model) to study the fracture behavior of FGMs with arbitrarily varying properties. In this model, constant elastic modulus in each sub-layer is assumed. This implies that the material properties are still discontinuous at the sub-interfaces. To overcome the disadvantages of the models mentioned before, Wang and Gross (2000) recently suggested a new multi-layered model for the static and dynamic fracture analysis of FGMs with properties varying arbitrarily under anti-plane deformation. Based on the fact that an arbitrary curve can be approached by a series of continuous piecewise linear curves, the FGMs are modeled as a multi-layered medium with the elastic modulus varying linearly in each sub-layer and continuous on the sub-interfaces. Later Wang et al. (2003) and Huang et al. (2002) presented detailed calculations to demonstrate the advantages of the model for the anti-plane deformation. In this paper, we will extend the new multi-layered model to an FGM interfacial zone under plane deformation. As we know, the mathematics involved in the plane problems is much more difficult.

2. Formulation of the problem

2.1. The new multi-layered model for fracture analysis of FGMs and basic equations

Consider a functionally graded interfacial zone of thickness h_0 sandwiched between two homogeneous half-planes. A through crack of length $2c$ lies parallel to the interface in the interfacial zone as shown in Fig. 1a. Generally the shear modulus $\mu(y)$ and the Poisson's ratio $\upsilon(y)$ of the coating may be described by two arbitrary continuous functions of y with boundary values $\mu(h_0) = \mu_0$, $\upsilon(h_0) = \upsilon_0$, $\mu(0) = \mu^*$ and $\upsilon(0) = \upsilon^*$

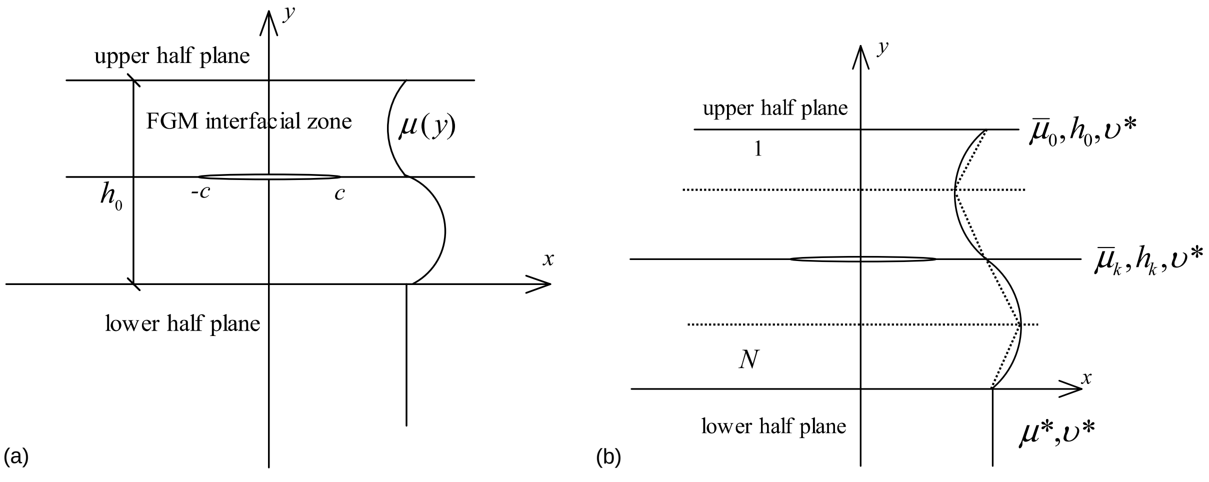

Fig. 1. A FGM interfacial zone sandwiched between two homogeneous half-planes (a); and the new multi-layered model for the FGM interfacial zone (b).

where μ^* and υ^* are, respectively, the shear modulus and Poisson's ratio of the lower homogenous half-plane, and μ_0 and υ_0 are those of the upper half-plane. However, previous studies (see Chen and Erdogan, 1996; Wu and Erdogan, 1996; Choi, 1997) have shown that the influence of the variation in Poisson's ratio on stress intensity factors is rather insignificant. Therefore, as they did, we assume the Poison's ratio is the same constant for both the graded interfacial zone and the two half-planes. Considering the fact that an arbitrary curve can be approximated by a continuous piecewise linear curve, we develop a new multi-layered model as shown in Fig. 1b. In this model, the graded interfacial zone is divided into N sub-layers with the crack on the kth sub-interface (k may be any integer between 1 and N). The shear modulus in the graded zone varies linearly in each sub-layer and is continuous at the sub-interfaces, i.e.,

$$\mu(y) \approx \mu_j(y) = \bar{\mu}_j \cdot (a_j + b_j y), \quad h_j < y < h_{j-1}, \quad j = 1, 2, \ldots, N, \tag{1}$$

where $\bar{\mu}_j$ is equal to the real value of the shear modulus at the sub-interface, $y = h_j$, i.e., $\bar{\mu}_j = \mu_j(h_j) = \mu(h_j)$ which leads to

$$a_j = \frac{h_{j-1} - h_j \bar{\mu}_{j-1}/\bar{\mu}_j}{h_{j-1} - h_j}, \quad b_j = \frac{\bar{\mu}_{j-1}/\bar{\mu}_j - 1}{h_{j-1} - h_j}. \tag{2}$$

If one introduces Airy stress function ϕ_j $(j = 0, \ldots, N+1)$, it can be easily found that the elastic behavior of the sub-layers of the graded zone under plane strain state is governed by the following compatibility equation

$$\frac{1-\upsilon^*}{2\mu_j(y)}\nabla^4\phi_j - \frac{\bar{\mu}_j b_j (1-\upsilon^*)}{\mu_j^2(y)}\left(\frac{\partial^3\phi_j}{\partial y^3} + \frac{\partial^3\phi_j}{\partial x^2 \partial y}\right) + \frac{[\bar{\mu}_j b_j]^2}{\mu_j^3(y)}\left[(1-\upsilon^*)\frac{\partial^2\phi_j}{\partial y^2} - \upsilon^*\frac{\partial^2\phi_j}{\partial x^2}\right] = 0, \quad j = 1, \ldots, N, \tag{3}$$

while those for the two homogeneous half-planes are controlled by

$$\nabla^4\phi_0 = 0, \quad \nabla^4\phi_{N+1} = 0. \tag{4}$$

The present crack problem can be viewed as the superposition of the following two sub-problems: (i) the system free of cracks is subjected to remote loading, inducing shear and tensile tractions $\sigma_1(x)$ and $\sigma_2(x)$ at $y = h_k$; (ii) the crack face is loaded under $-\sigma_1(x)$ and $-\sigma_2(x)$ without the remote loads. Since problem (i) contributes nothing to the singular fields at the crack tips, we will pay attention only to problem (ii) treating $-\sigma_1(x)$ and $-\sigma_2(x)$ as known functions. Further we denote the displacement jumps across the crack plane as Δu_{xk} and Δu_{yk}. Thus, the condition of the continuity of the displacements and stresses on the interfaces free of crack (i.e., $y = h_j$ $(j = 0, \ldots, N+1, j \neq k)$) can be stated as

$$u_{xj}(x, h_j) = u_{xj+1}(x, h_j), \tag{5}$$

$$u_{yj}(x, h_j) = u_{yj+1}(x, h_j), \tag{6}$$

$$\sigma_{xyj}(x, h_j) = \sigma_{xyj+1}(x, h_j), \tag{7}$$

$$\sigma_{yyj}(x, h_j) = \sigma_{yyj+1}(x, h_j), \tag{8}$$

and on the crack plane, we have

$$u_{xk}(x, h_k) - u_{xk+1}(x, h_k) = \Delta u_{xk}(x) H(c^2 - x^2), \tag{9}$$

$$u_{yk}(x, h_k) - u_{yk+1}(x, h_k) = \Delta u_{yk}(x) H(c^2 - x^2), \tag{10}$$

$$\sigma_{xyk}(x, h_k) = \sigma_{xyk+1}(x, h_k), \quad |x| > c, \qquad \sigma_{xyk}(x, h_k) = -\sigma_1(x), \quad |x| \leqslant c, \tag{11}$$

$$\sigma_{yyk}(x,h_k)=\sigma_{yyk+1}(x,h_k),\quad |x|>c,\qquad \sigma_{yyk}(x,h_k)=-\sigma_2(x),\quad |x|\leqslant c, \tag{12}$$

with $H(\ )$ being the Heaviside function.

2.2. Transfer matrix and dual integral equations

Subject Eq. (3) to Fourier integral transform with respect to x, then it becomes

$$\frac{1-\upsilon^*}{2\mu_j(y)}\left(\frac{\mathrm{d}^2}{\mathrm{d}y^2}-s^2\right)^2\tilde{\phi}_j-\frac{\bar{\mu}_jb_j(1-\upsilon^*)}{\mu_j^2(y)}\left(\frac{\mathrm{d}^2}{\mathrm{d}y^2}-s^2\right)\frac{\mathrm{d}\tilde{\phi}_j}{\mathrm{d}y}+\frac{[\bar{\mu}_jb_j]^2}{\mu_j^3(y)}\left[(1-\upsilon^*)\frac{\mathrm{d}^2\tilde{\phi}_j}{\mathrm{d}y^2}+\upsilon^*s^2\tilde{\phi}_j\right]=0, \tag{13}$$

with '$\sim$' standing for the Fourier integral transform. If the following substitutes are introduced:

$$\xi_j=2s(a_j+b_jy)/b_j,\quad \tilde{\phi}_j(\xi_j)=f_j(\xi_j)\xi_j/2, \tag{14}$$

Eq. (13) then is reduced to

$$\frac{\mathrm{d}^4f_j}{\mathrm{d}\xi_j^4}+\frac{2}{\xi_j}\frac{\mathrm{d}^3f_j}{\mathrm{d}\xi_j^3}-\left(\frac{1}{2}+\frac{4}{\xi_j^2}\right)\frac{\mathrm{d}^2f_j}{\mathrm{d}\xi_j^2}+\left(\frac{4}{\xi_j^3}-\frac{1}{2\xi_j}\right)\frac{\mathrm{d}f_j}{\mathrm{d}\xi_j}+\left(\frac{1}{16}+\frac{1-\gamma^2}{\xi_j^2}\right)f_j=0, \tag{15}$$

where $\gamma=[(1-2\upsilon^*)/(2-2\upsilon^*)]^{1/2}$. The general solutions for Eq. (15) are Whittaker functions (Slater, 1960), i.e.,

$$f_j(\xi_j)=A_{j1}W_{\gamma,1.5}(\xi_j)+A_{j2}W_{-\gamma,1.5}(\xi_j)+A_{j3}W_{\gamma,-1.5}(\xi_j)+A_{j4}W_{-\gamma,-1.5}(\xi_j), \tag{16}$$

from which, together with Eq. (14), we obtain the transformed Airy stress function in each sub-layer as

$$\begin{aligned}\tilde{\phi}_j(\xi_j)&=\left[A_{j1}W_{\gamma,1.5}(\xi_j)+A_{j2}W_{-\gamma,1.5}(\xi_j)+A_{j3}W_{\gamma,-1.5}(\xi_j)+A_{j4}W_{-\gamma,-1.5}(\xi_j)\right]\xi_j/2\\ &\stackrel{d.}{=}A_{j1}\tilde{\phi}_{j1}(\xi_j)+A_{j2}\tilde{\phi}_{j2}(\xi_j)+A_{j3}\tilde{\phi}_{j3}(\xi_j)+A_{j4}\tilde{\phi}_{j4}(\xi_j).\end{aligned} \tag{17}$$

The transformed displacement and stress components consequently can be written in the following matrix form

$$\{S_j(y)\}=[T_j(y)]\{A_j\}=[T_{j1}(y),T_{j2}(y),T_{j3}(y),T_{j4}(y)]\{A_j\}, \tag{18}$$

where

$$\{S_j\}=[\tilde{u}_{xj},\tilde{u}_{yj},\tilde{\sigma}_{xyj},\tilde{\sigma}_{yyj}]^{\mathrm{T}},$$

$$\{A_j\}=[A_{j1},A_{j2},A_{j3},A_{j4}]^{\mathrm{T}},$$

$$T_{jl}(y)=[T_{jl1}(y),T_{jl2}(y),T_{jl3}(y),T_{jl4}(y)]^{\mathrm{T}},$$

with

$$T_{jl1}(y)=\frac{-\mathrm{i}}{2\mu_j(y)s}(1-\upsilon^*)\frac{\mathrm{d}^2\tilde{\phi}_{jl}(y)}{\mathrm{d}y^2}-\frac{\mathrm{i}\upsilon^*s}{2\mu_j(y)}\tilde{\phi}_{jl}(y),$$

$$T_{jl2}(y)=\frac{1-\upsilon^*}{2\mu_j(y)s^2}\frac{\mathrm{d}^3\tilde{\phi}_{jl}(y)}{\mathrm{d}y^3}-\frac{\bar{\mu}_jb_j(1-\upsilon^*)}{2\mu_j^2(y)s^2}\frac{\mathrm{d}^2\tilde{\phi}_{jl}(y)}{\mathrm{d}y^2}-\frac{2-\upsilon^*}{2\mu_j(y)}\frac{\mathrm{d}\tilde{\phi}_{jl}(y)}{\mathrm{d}y}-\frac{\bar{\mu}_jb_j\upsilon^*}{2\mu_j^2(y)}\tilde{\phi}_{jl}(y),$$

$$T_{jl3}(y)=-\mathrm{i}s\frac{\mathrm{d}\tilde{\phi}_{jl}(y)}{\mathrm{d}y},\quad T_{jl4}(y)=-s^2\tilde{\phi}_{jl}(y),\quad l=1,2,3,4.$$

The superscript "T" in the above equations denotes the transposition of a matrix. Eq. (4) for the homogeneous half-planes can be solved similarly. For simplicity, we directly write the displacements and stresses in two half-planes as

$$\{S_0(y)\} = [T_0(y)]\{B_1\}\{A_0\}, \quad \{S_{N+1}\} = [T_{N+1}(y)]\{B_2\}\{A_N\}, \tag{19}$$

where

$$\{B_1\} = \begin{bmatrix} 1 & 0 & 0 & 0 \\ 0 & 1 & 0 & 0 \end{bmatrix}^{\mathrm{T}}, \quad \{B_2\} = \begin{bmatrix} 0 & 0 & 1 & 0 \\ 0 & 0 & 0 & 1 \end{bmatrix}^{\mathrm{T}},$$

$$\{A_0\} = [A_{01}, A_{02}]^{\mathrm{T}}, \quad \{A_N\} = [A_{N1}, A_{N2}]^{\mathrm{T}},$$

$$[T_j(y)] = [T_{j1}(y), T_{j2}(y)], \quad (j = 0 \text{ or } N+1),$$

with

$$[T_{j1}(y)] = \begin{bmatrix} s/2\mathrm{i}\mu_j & |s|/2\mu_j & -\mathrm{i}s & -s^2 \\ [ys - 2(1-\upsilon^*)|s|/s]/2\mathrm{i}\mu_j & (1 - 2\upsilon^* + y|s|)/2\mu_j & -\mathrm{i}s(1 - y|s|) & -s^2 y \end{bmatrix}^{\mathrm{T}} \exp(-|s|y),$$

$$[T_{j2}(y)] = \begin{bmatrix} s/2\mathrm{i}\mu_j & -|s|/2\mu_j & -\mathrm{i}s & -s^2 \\ [ys + 2(1-\upsilon^*)|s|/s]/2\mathrm{i}\mu_j & (1 - 2\upsilon^* - y|s|)/2\mu_j & -\mathrm{i}s(y|s| + 1) & -s^2 y \end{bmatrix}^{\mathrm{T}} \exp(|s|y),$$

and $\mu_j = \mu_0$ for $j = 0$ and $\mu_j = \mu^*$ for $j = N+1$. Making use of Eqs. (5)–(12), one may have

$$\{S_j\} - \{S_{j+1}\} = \{\Delta S_k\}\delta_{kj}, \quad y = h_j, \quad j = 1, 2, \ldots, N, \tag{20}$$

in which δ_{kj} is the Kronecker delta and $\{\Delta S_k\} = [\Delta\tilde{u}_{xk}, \Delta\tilde{u}_{yk}, 0, 0]^{\mathrm{T}}$ with $\Delta\tilde{u}_{xk}$ and $\Delta\tilde{u}_{yk}$ being the Fourier transforms of the jumps of the displacements across the crack face.

Eq. (20) in essence is a recurrence relation that, in combination with Eqs. (18) and (19), can yield $\{A_j\}$ in terms of $\{\Delta S_k\}$

$$\{A_j\} = ([\overline{L}_{jk}] + [\overline{K}_{jk}]H(j - k - 1))\{\Delta S_k\}, \quad j = 1, 2, \ldots, N, \tag{21}$$

where

$$[W_j] = [T_j(h_j)]^{-1}[T_{j+1}(h_j)], \quad [\overline{W}] = \{B_1\}\{B_1\}^{\mathrm{T}} - [\overline{W}_N]\{B_2\}\{B_2\}^{\mathrm{T}},$$

$$[L_k] = [\overline{W}_k][T_{k+1}(h_k)]^{-1}, \quad [\overline{W}_j] = [W_0][W_1]\cdots[W_j], \quad [\overline{W}_0] = [W_0],$$

$$[\overline{L}_{jk}] = [\overline{W}_{j-1}]^{-1}[\overline{E}_k], \quad [\overline{K}_{jk}] = -[\overline{W}_{j-1}]^{-1}[L_k], \quad [\overline{E}_k] = \{B_1\}\{B_1\}^{\mathrm{T}}[\overline{W}]^{-1}[L_k],$$

where $[T_j(h_j)]^{-1}$ refers to the inversion of the 4×4 matrix $[T_j(h_j)]$. Upon substituting of Eq. (21) into (18) and applying the inverse Fourier transform, one obtains

$$\{u_{xj}, u_{yj}, \sigma_{xyj}, \sigma_{yyj}\}^{\mathrm{T}} = \frac{1}{2\pi}\int_{-\infty}^{\infty} [M_{jk}]\{\Delta S_k\}\exp(\mathrm{i}sx)\,\mathrm{d}s, \quad j = 1, 2, \ldots, N, \tag{22}$$

where we have denoted

$$[M_{jk}] = [T_j(y)]([\overline{L}_{jk}] + [\overline{K}_{jk}]H(j - k - 1)), \tag{23}$$

which is none other than the transfer matrix for the multiple layered medium. Extracting the stress components from Eq. (22), we have

$$\{\sigma_{xyj},\sigma_{yyj}\}^{\mathrm{T}}=\frac{1}{2\pi}\int_{-\infty}^{\infty}\bar{m}(s,y)\{\Delta\tilde{u}_{xk},\Delta\tilde{u}_{yk}\}^{\mathrm{T}}\exp(\mathrm{i}sx)\,\mathrm{d}s,\quad j=1,2,\ldots,N,\tag{24}$$

where $\bar{m}(s,y)=[B_2]^{\mathrm{T}}[M_{jk}][B_1]$. Satisfaction of Eq. (24) with the boundary conditions (11) and (12) gives

$$\frac{1}{2\pi}\int_{-\infty}^{\infty}\bar{m}(s,h_k)\{\Delta\tilde{u}_{xk},\Delta\tilde{u}_{yk}\}^{\mathrm{T}}\exp(\mathrm{i}sx)\,\mathrm{d}s=-\{\sigma_1(x),\sigma_2(x)\}^{\mathrm{T}},\quad |x|\leqslant c.\tag{25}$$

The single-valued condition for displacement components yields

$$\int_{-\infty}^{\infty}\{\Delta\tilde{u}_{xk},\Delta\tilde{u}_{yk}\}^{\mathrm{T}}\exp(\mathrm{i}sx)\,\mathrm{d}s=0,\quad |x|>c,\tag{26}$$

Eqs. (25) and (26) are dual integral equations for the present problem.

2.3. Cauchy singular integral equations

If the following dislocation density functions are introduced:

$$\psi_1(x)=\frac{\partial}{\partial x}(\Delta u_{xk}),\quad \psi_2(x)=\frac{\partial}{\partial x}(\Delta u_{yk}),\quad |x|\leqslant c,\tag{27}$$

Eqs. (25) and (26) can be rewritten as

$$\frac{1}{2\pi\mathrm{i}}\int_{-\infty}^{\infty}s^{-1}\bar{m}(s,h_k)\int_{-c}^{c}\{\psi_1(v),\psi_2(v)\}^{\mathrm{T}}\exp[\mathrm{i}s(x-v)]\,\mathrm{d}u\,\mathrm{d}s=-\{\sigma_1(x),\sigma_2(x)\}^{\mathrm{T}},\quad |x|\leqslant c,\tag{28}$$

$$\int_{-c}^{c}\{\psi_1(v),\psi_2(v)\}^{\mathrm{T}}\,\mathrm{d}v=0.\tag{29}$$

It can be proved that $s^{-1}\bar{m}(s,h_k)$ possesses the following asymptotic behavior if one resorts to the behavior of Whittaker functions (Slater, 1960):

$$\lim_{s\to+\infty}s^{-1}\bar{m}(s,h_k)=\begin{bmatrix}-\alpha_1 & 0\\ 0 & -\alpha_1\end{bmatrix},\tag{30}$$

with $\alpha_1=\bar{\mu}_k/(2-2v^*)$. Furthermore the elements of $\bar{m}(s,h_k)$ behave as

$$\bar{m}_{jl}(-s)=(-1)^{j+l}\bar{m}_{jl}(s),\quad j,l=1,2.\tag{31}$$

Then, using the relation

$$\int_{-\infty}^{+\infty}\mathrm{sgn}(s)\exp[\mathrm{i}s(v-x)]\,\mathrm{d}s=\frac{2\mathrm{i}}{v-x},\tag{32}$$

we convert Eq. (25) into the following Cauchy singular integral equations:

$$\int_{-c}^{c}\left\{\begin{bmatrix}\alpha_1/(v-x) & 0\\ 0 & \alpha_1/(v-x)\end{bmatrix}+\begin{bmatrix}Q_{11}(v,x) & Q_{12}(v,x)\\ Q_{21}(v,x) & Q_{22}(v,x)\end{bmatrix}\right\}\left\{\begin{matrix}\psi_1(v)\\ \psi_2(v)\end{matrix}\right\}\mathrm{d}u$$
$$=-\pi\left\{\begin{matrix}\sigma_1(x)\\ \sigma_2(x)\end{matrix}\right\},\quad |x|\leqslant c,\tag{33}$$

where

$$Q_{jl}(v,x)=-\int_0^{\infty}[s^{-1}\bar{m}_{jl}(s)+\alpha_1]\sin[s(v-x)]\,\mathrm{d}s,\quad j=l,$$

$$Q_{jl}(v,x) = \int_0^\infty (\mathrm{i}s)^{-1}\bar{m}_{jl}(s)\cos[s(v-x)]\,\mathrm{d}s, \quad j \neq l.$$

It can be proved that $\bar{m}_{12}(s)$ and $\bar{m}_{21}(s)$ have the asymptotic behavior

$$\lim_{s\to\infty} \bar{m}_{12}(s) = -\lim_{s\to\infty} \bar{m}_{21}(s) = -\alpha_2, \tag{34}$$

with $\alpha_2 = \mathrm{i}(\bar{\mu}_{k-1}b_{k-1} + \bar{\mu}_k b_k)/(8-8v^*)$. So $Q_{12}(v,x)$ and $Q_{21}(v,x)$ can be rewritten as

$$Q_{jl}(v,x) = \int_0^{s_1} (\mathrm{i}s)^{-1}\bar{m}_{jl}(s)\cos[s(v-x)]\,\mathrm{d}s + \int_{s_1}^\infty (\mathrm{i}s)^{-1}[\bar{m}_{jl}(s) - (-1)^j\alpha_2]\cos[s(v-x)]\,\mathrm{d}s,$$
$$+\,\mathrm{i}(-1)^j\alpha_2 \int_0^{|s_1(v-x)|} (\cos t -)t^{-1}\,\mathrm{d}t$$

where s_1 is a positive constant to be determined by numerical tests and γ_0 is the Euler's constant. It is worth pointing out that if v^* in all above equations is replaced with $v^*/(1+v^*)$, we can get the formulation for the plane stress-state problem.

Eq. (25) together with (21) can be numerically solved by the method of Erdogan and Gupta (1972). Noting that the dislocation density functions have the square-root singularity at the crack tips, we can express them as

$$\psi_1(v) = \frac{f_1(v)}{\sqrt{1-(v/c)^2}}, \quad \psi_2(v) = \frac{f_2(v)}{\sqrt{1-(v/c)^2}}. \tag{35}$$

Discretize v and x in the following manner:

$$v_l = c\cos\frac{\pi}{2M}(2l-1), \quad l = 1,\ldots,M, \tag{36}$$

$$x_r = c\cos\frac{\pi r}{M}, \quad r = 1,\ldots,M-1, \tag{37}$$

and then we have

$$\frac{c}{M}\sum_{l=1}^{M}\left\{\frac{\alpha_1 f_j(v_l)}{v_l - x_r} + \sum_{n=1}^{2} f_n(v_l)Q_{jn}(v_l,x_r)\right\} = -\sigma_j(x_r), \quad j = 1,2, \tag{38}$$

$$\frac{1}{M}\sum_{1}^{M} f_j(v_l) = 0, \quad j = 1,2. \tag{39}$$

The stress intensity factors (SIFs) at the crack tips are defined as

$$K_{\mathrm{I}}^{\pm} = \lim_{x\to\pm c}\sqrt{2|x\mp c|}\,\sigma_{yy}(x,h_k), \quad K_{\mathrm{II}}^{\pm} = \lim_{x\to\pm c}\sqrt{2|x\mp c|}\,\sigma_{xy}(x,h_k), \tag{40}$$

which can be calculated by

$$K_{\mathrm{I}}^{\pm} = \mp\alpha_1\sqrt{c}f_2(\pm c), \quad K_{\mathrm{II}}^{\pm} = \mp\alpha_1\sqrt{c}f_1(\pm c). \tag{41}$$

3. Numerical examples and discussion

To verify the effectiveness of the present new model, we first consider the case that the shear modulus of the functionally graded coating can be described by Erdogan's model, i.e.,

$$\mu(y) = \mu^* \exp(\beta y), \tag{42}$$

where $\beta = \log(\mu_0/\mu^*)/h_0$. Throughout the paper the Poisson's ratio is taken as $\upsilon^* = 0.3$ and either $\sigma_1(x)$ or $\sigma_2(x)$ is set to be a constant and equal to σ_0. In this case, the crack problem can be solved by directly using Erdogan's model yielding more accurate results. In order to solve the problem by using the present new model, we have to determine how many sub-layers are necessary for the results to be sufficiently accurate. To this end, we have calculated the SIFs of a midline crack (i.e., $h_k = h_0/2$) with $\mu^*/\mu_0 = 1.88/0.45$, $c/h_0 = 1.0$ and 5.0 for different values of N under shear loading. Results are given in Table 1 where the SIFs have been normalized by $\sigma_0 c^{1/2}$. From Table 1, one can see that with the increase of N, the results are increasingly close to each other. And the results with $N = 4$ or 6 may be considered sufficiently accurate. So for this example, we will choose the number of the sub-layers to be 6.

Figs. 2 and 3 present the SIFs of a midline crack obtained by the present model, Erdogan's model and PWML model with $N = 6$ as a variation of c/h_0 for $\mu^*/\mu_0 = 20$ under normal and shear loading respectively. For the solution process of Erdogan's model, refer to Choi et al. (1998) or Shbeeb and Binienda (1999), while for that of the PWML model, refer to Wang et al. (2000) or Itou (2001). Figs. 2 and 3 show clearly that the results of the present model (the scattered crosses) are in good agreement with those of the Erdogan's model (the solid line), while those of the PWML model (the scattered squares) deviate from them considerably. So we may conclude that the present model is more efficient than the PWML model, which can be further verified from Figs. 4 and 5 where the SIFs of an interface crack (i.e., $h_k = 0$) are given as a variation of c/h_0 for $\mu^*/\mu_0 = 20$ under normal and shear loading respectively.

Table 1
Effect of N on SIFs of a midline crack in a FGM interfacial zone under shear loading with $\mu^*/\mu_0 = 1.88/0.45$ (exponential variation)

N	$c/h_0 = 1.0$		$c/h_0 = 5.0$	
	$K_I/\sigma_0 c^{1/2}$	$K_{II}/\sigma_0 c^{1/2}$	$K_I/\sigma_0 c^{1/2}$	$K_{II}/\sigma_0 c^{1/2}$
2	0.1551846	0.9964912	0.2211133	1.0356900
4	0.1545255	1.0065845	0.2206882	1.0365365
6	0.1545192	1.0091211	0.2235252	1.0495061
8	0.1545104	1.0099517	0.2240124	1.0518444
10	0.1545057	1.0103222	0.2241178	1.0523903

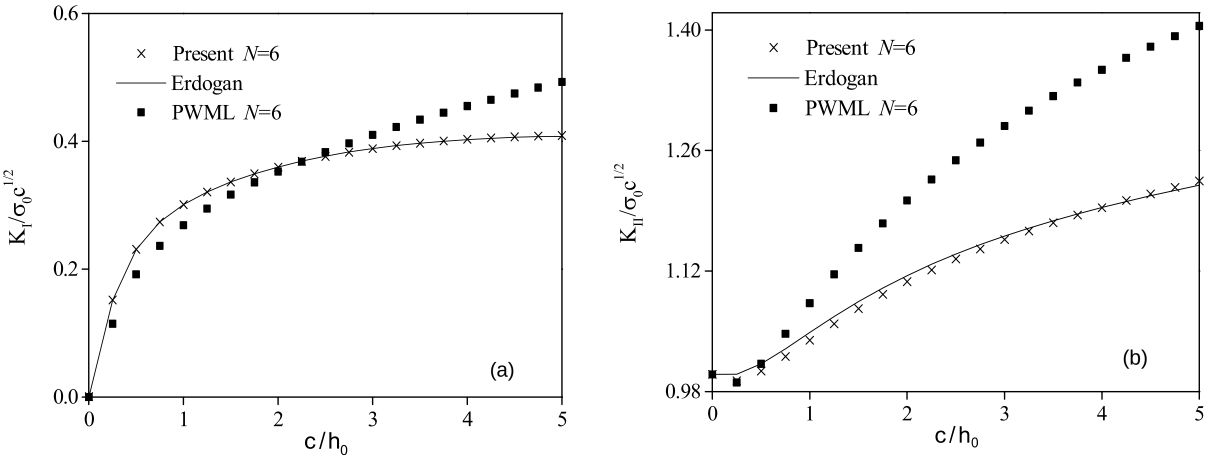

Fig. 2. Normalized SIFs for a midline crack in a FGM interfacial zone under shear loading, exponential variation. (a) Mode I SIFs; and (b) Mode II SIFs.

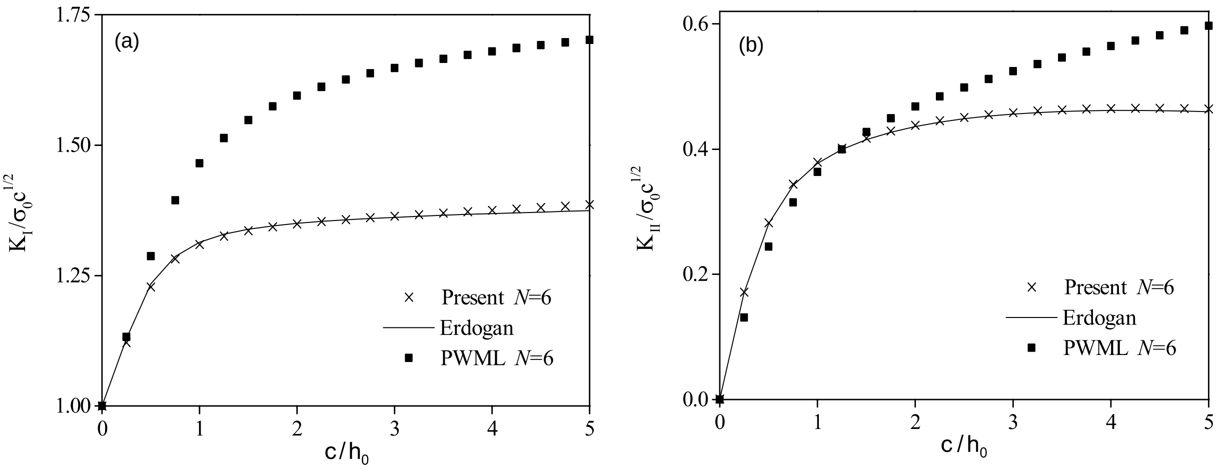

Fig. 3. Normalized SIFs for a midline crack in a FGM interfacial zone under normal loading, exponential variation. (a) Mode I SIFs; and (b) Mode II SIFs.

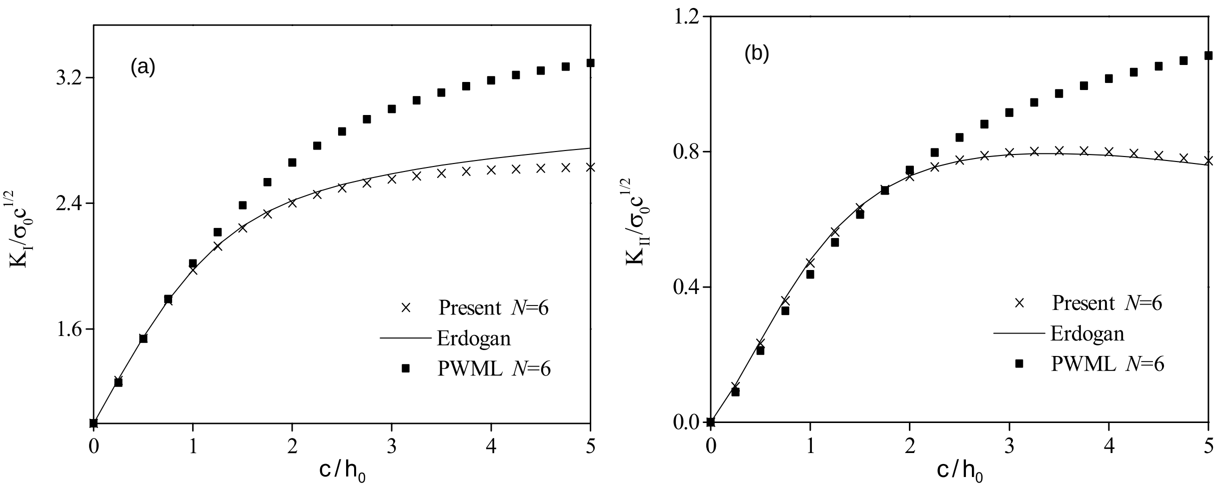

Fig. 4. Normalized SIFs for an interface crack in a FGM interfacial zone under normal loading, exponential variation. (a) Mode I SIFs; and (b) Mode II SIFs.

As mentioned before, one of the advantages of the present model over other models is that it can be used for the FGMs with shear modulus varying arbitrarily and involves no discontinuity of the properties. Therefore, as an example, we consider the shear modulus of the interfacial zone varying in the sinusoidal form:

$$\mu(y) = \mu^* + (\mu_0 - \mu^*)\sin(\pi y/2h_0). \tag{43}$$

Taking $\mu^*/\mu_0 = 1.88/0.45$, we have calculated the SIFs of a midline crack for different N under shear loading. The results are listed in Table 2. It is shown clearly that the results for $N = 6$ can be reckoned sufficiently accurate. Therefore we choose $N = 6$ in the following calculation. The SIFs for a midline crack

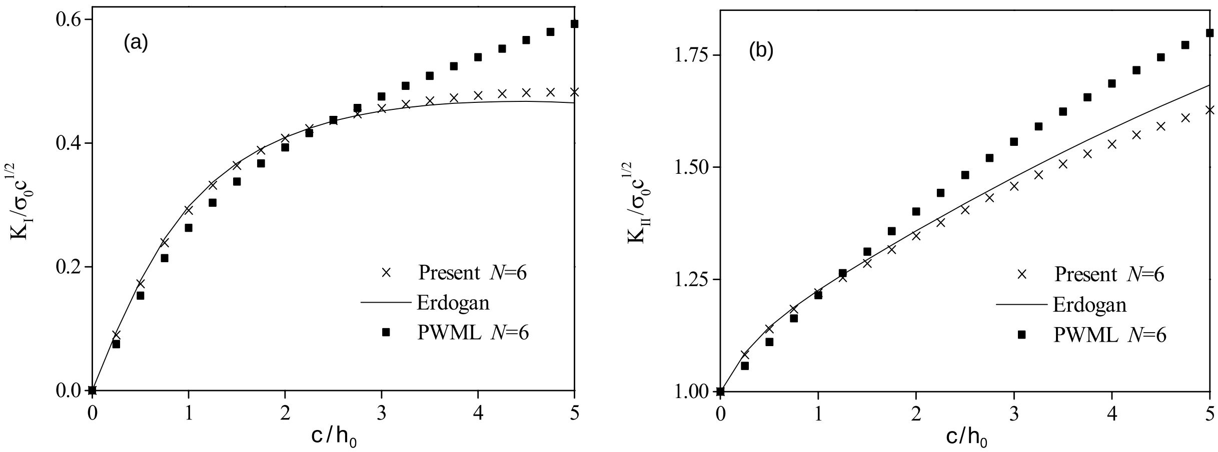

Fig. 5. Normalized SIFs for an interface crack in a FGM interfacial zone under shear loading, exponential variation. (a) Mode I SIFs; and (b) Mode II SIFs.

Table 2
Effect of N on SIFs of a midline crack in a FGM interfacial zone under shear loading with $\mu^*/\mu_0 = 1.88/0.45$ (sinusoidal variation)

N	$c/h_0 = 1.0$		$c/h_0 = 5.0$	
	$K_I/\sigma_0 c^{1/2}$	$K_{II}/\sigma_0 c^{1/2}$	$K_I/\sigma_0 c^{1/2}$	$K_{II}/\sigma_0 c^{1/2}$
2	0.1538333	0.9838516	0.2175648	1.0146287
4	0.1589588	1.0013367	0.2210860	1.0258443
6	0.1599181	1.0049592	0.2216323	1.0282008
8	0.1602642	1.0062614	0.2217993	1.0289274
10	0.1604306	1.0068762	0.2219043	1.0293858

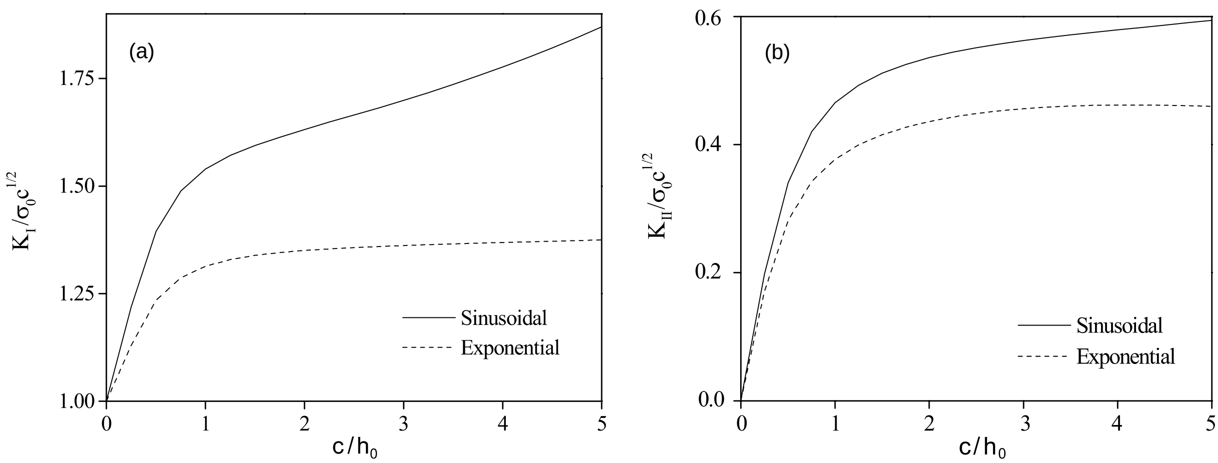

Fig. 6. Normalized SIFs for a midline crack in a FGM interfacial zone under normal loading, sinusoidal variation in comparison with the exponential variation. (a) Mode I SIFs; and (b) Mode II SIFs.

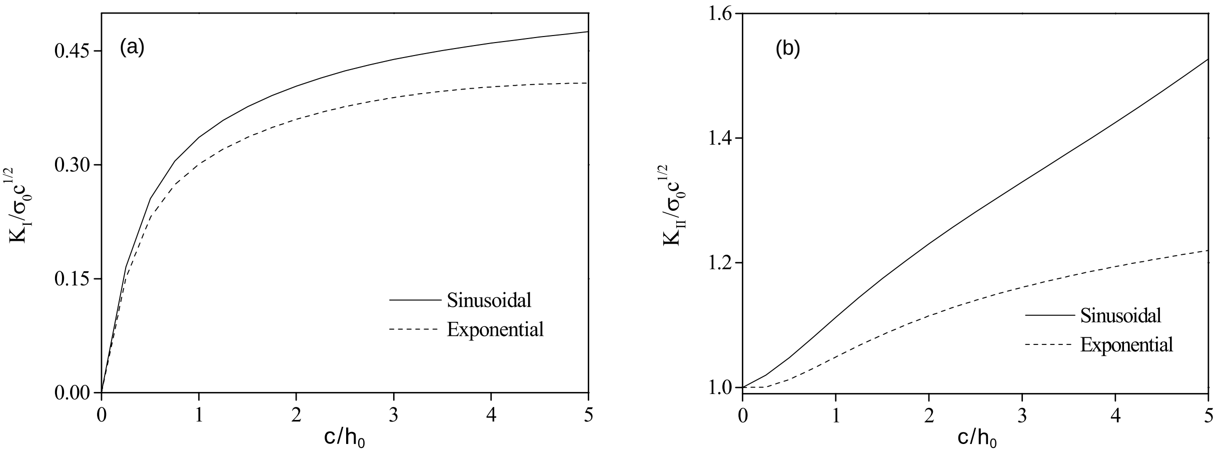

Fig. 7. Normalized SIFs for a midline crack in a FGM interfacial zone under shear loading, sinusoidal variation in comparison with the exponential variation. (a) Mode I SIFs; and (b) Mode II SIFs.

under normal and shear loading with $\mu^*/\mu_0 = 20$ have been plotted in Figs. 6 and 7 respectively. For the purpose of comparison, results for the exponential shear modulus are replotted by the dashed lines. It is shown that the SIFs for the two forms of the shear modulus are different from each other. This is due to the different variations of the shear modulus in the functionally graded interfacial zone. To further shed light on this, we have calculated the SIFs for an interface crack under normal and shear loading. The results are demonstrated in Figs. 8 and 9 which show clearly that the SIFs of the two forms of the shear modulus are still different from each other especially when the crack is under shear loading (see Fig. 9b). The values of the shear modulus for the two forms in this case are identical on the interface, so we can conclude that the form of the shear modulus can influence the SIFs much, which necessitates the present model for fracture analysis of FGMs with arbitrarily varying properties.

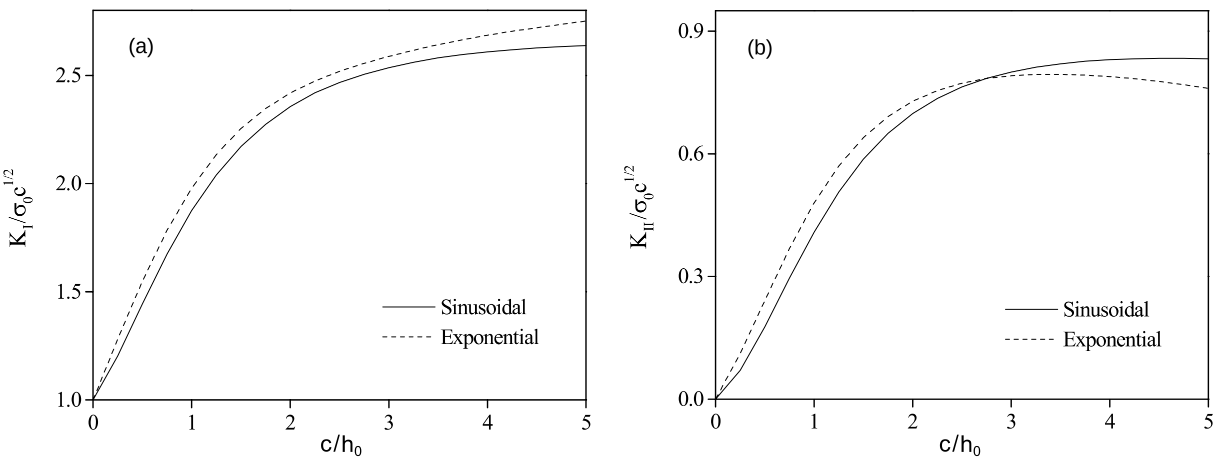

Fig. 8. Normalized SIFs for an interface crack in a FGM interfacial zone under normal loading, sinusoidal variation in comparison with the exponential variation. (a) Mode I SIFs; and (b) Mode II SIFs.

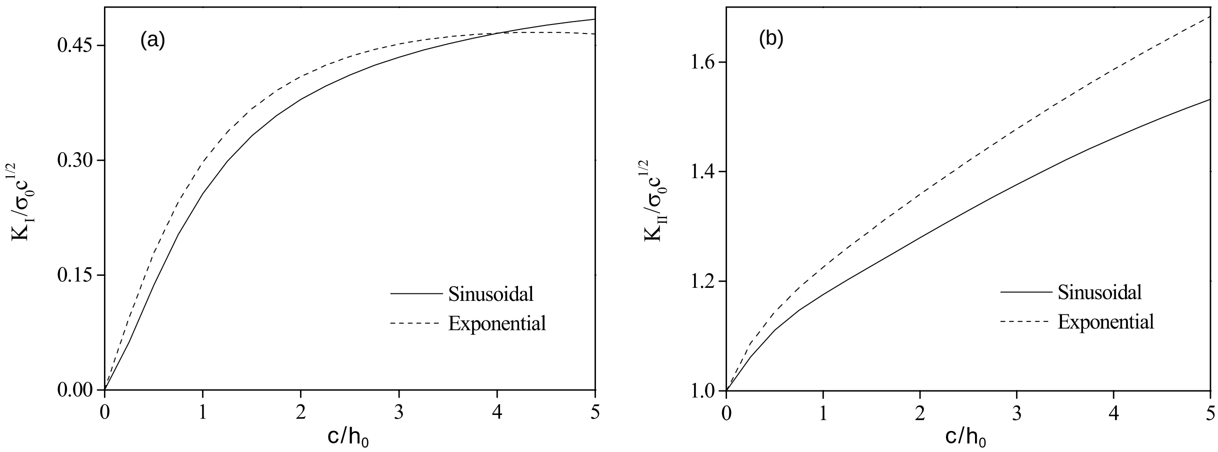

Fig. 9. Normalized SIFs for an interface crack in a FGM interfacial zone under shear loading, sinusoidal variation in comparison with the exponential variation. (a) Mode I SIFs; and (b) Mode II SIFs.

4. Concluding remarks

In this paper, we have generalized the multi-layered model for anti-plane fracture analysis of FGMs with arbitrary form of shear modulus developed by Wang and Gross (2000) and Wang et al. (2003) to the plane deformation. Taking a functionally graded interfacial zone bonded to two homogeneous half-planes as an example, we have calculated the SIFs of a midline crack and an interface crack for the shear modulus of the interfacial zone varying in an exponential manner and in a sinusoidal manner. From the numerical results, we could find:

(1) The present model is very efficient in solving the crack problems of the FGMs. Generally 4–6 sub-layers can yield sufficiently accurate results.
(2) The advantage of the present model over Erdogan's model lies in the fact that the present model can be used to fracture analysis of the FGMs with arbitrarily varying elastic properties.
(3) The present model also has advantages over the PWML-model. On one hand, the present model involves no discontinuities of the material properties while the PWML model does. On the other hand, the present model is more efficient than the PWML model in simulating the FGMs because the present model requires fewer sub-layers than the PWML-model to yield sufficiently accurate results.
(4) The form of shear modulus can influence the SIFs of cracks in the functionally graded interfacial zone.

Acknowledgements

The work is partially supported by the National Science Fund for Distinguished Young Scholars under grant no. 10025211 and Doctoral Science Fund of MOE under grant no. 20020004005.

References

Chen, Y.F., Erdogan, F., 1996. The interface crack problem for a nonhomogeneous coating bonded to a homogeneous substrate. J. Mech. Phys. Solids 44, 771–787.
Choi, H.J., 1997. A periodic array of cracks in a functionally graded nonhomogeneous medium loaded under in-plane normal and shear. Int. J. Fract. 88, 107–128.

Choi, H.J., Lee, K.Y., Jin, T.E., 1998. Colinear cracks in a layered half-plane with a graded nonhomogeneous interfacial zone—Part I: Mechanical response. Int. J. Fract. 94, 103–122.

Delale, F., Erdogan, F., 1983. The crack problem for a nonhomogeneous plane. ASME J. Appl. Mech. 50, 609–614.

Delale, F., Erdogan, F., 1988. On the mechanical modeling of the interfacial region in bonded half-plane. ASME J. Appl. Mech. 55, 317–324.

Eischen, J.W., 1987. Fracture of nonhomogeneous materials. Int. J. Fract. 34, 3–22.

Erdogan, F., Gupta, G.D., 1972. On the numerical solution of singular integral equations. Q. Appl. Math. 29, 525–534.

Erdogan, F., Kaya, A.C., Joseph, P.F., 1991. The mode-III crack problem in bonded materials with a nonhomogeneous interfacial zone. ASME J. Appl. Mech. 58, 419–427.

Ergüven, M.E., Gross, D., 1999. On the penny-shaped crack in inhomogeneous elastic materials under normal extension. Int. J. Solids Struct. 36, 1869–1882.

Fildis, H., Yahsi, O.S., 1996. The axisymmetric crack problem in a nonhomogeneous interfacial region between homogeneous half-spaces. Int. J. Fract. 78, 139–164.

Fildis, H., Yahsi, O.S., 1997. The mode III axisymmetric crack problem in a non-homogeneous interfacial region between homogeneous half-spaces. Int. J. Fract. 85, 35–45.

Gao, H., 1991. Fracture analysis of nonhomogeneous materials via a moduli-perturbation approach. Int. J. Solids Struct. 27, 1663–1682.

Huang, G.Y., Wang, Y.S., Gross, D., 2002. Fracture analysis of functionally graded coatings: antiplane deformation. Eur. J. Mech. A/Solids 21, 391–400.

Itou, S., 2001. Transient dynamic stress intensity factors around a crack in a nonhomogeneous interfacial layer between two dissimilar elastic half-planes. Int. J. Solids Struct. 38, 3631–3645.

Jin, Z.H., Noda, N., 1994. Crack tip singular fields in nonhomogeneous materials. J. Appl. Mech. 61, 738–740.

Ozturk, M., Erdogan, F., 1993. Antiplane shear crack problem in bonded materials with a graded interfacial zone. Int. J. Eng. Sci. 31, 1641–1657.

Ozturk, M., Erdogan, F., 1995. An axisymmetrical crack in bonded materials with a nonhomogeneous interfacial zone under torsion. ASME J. Appl. Mech. 62, 116–125.

Ozturk, M., Erdogan, F., 1996. Axisymmetric crack problem in bonded materials with a graded interfacial region. Int. J. Solids Struct. 33, 193–219.

Shbeeb, N.I., Binienda, W.K., 1999. Analysis of an interface crack for a functionally graded strip sandwiched between two homogeneous layers of finite thickness. Eng. Fract. Mech. 64, 693–720.

Slater, L.J., 1960. Confluent Hypergeometric Functions. Cambridge University Press, Cambridge.

Wang, B.L., Han, J.C., Du, S.Y., 2000. Cracks problem for nonhomogeneous composite material subjected to dynamic loading. Int. J. Solids Struct. 37, 1251–1274.

Wang, X.Y., Wang, D., Zou, Z.Z., 1996. On the Griffith crack in a nonhomogeneous interlayer of adjoining two different elastic materials. Int. J. Fract. 79, R51–R56.

Wang, Y.S., Gross, D., 2000. Analysis of a crack in a functionally gradient interface layer under static and dynamic loading. Key Engng. Mater. 183–187, 331–336.

Wang, Y.S., Huang, G.Y., Gross, D., 2003. On the mechanical modeling of functionally graded interfacial zone with a Griffith crack: anti-plane deformation. ASME J. Appl. Mech., in press.

Wu, B.H., Erdogan, F., 1996. Crack problems in FGM layers under thermal stresses. J. Therm. Stresses 19, 237–265.